# Design and Analysis of a Bidirectional Hybrid DC Circuit Breaker Using AC Relays With Long Life Time

Ken King Man Siu, *Member, IEEE*, Carl Ngai Man Ho, *Senior Member, IEEE*, and Dong Li, *Student Member, IEEE*

***Abstract*—This article presented a new hybrid circuit breaker solution for using in dc microgrids. The proposed solution can offer a high-reliability protection feature for the dc microgrid with low conduction loss, bidirectional current flow, and galvanic isolation function. In the design, it is combined with a group of mechanical switches and semiconductors, where the mechanical switches handle the current conduction during normal operation and the semiconductors handle the breaker response during transient operation. The design fully utilizes the advantage of both types of switches and maximizes the performance and life time of the system. Throughout the design, it maintains only one mechanical switch in series with each power line; thereby, the high conductivity of the circuit breaker is maintained. At the same time, through the hybrid design, the electrical stress applied to the mechanical switch is eliminated. Thus, an effective and high-reliability solution is provided for the design of dc circuit breakers. The operation principle is explained in detail and the design guideline is provided. A 150/380 V and 15 A circuit breaker is successfully implemented, and the performance is experimentally verified, which shows good agreement with the theoretical findings.**

***Index Terms*—DC circuit breaker, microgrid relay, semiconductor application.**

## I. Introduction

THE development of smart grid brings a technological revolution from the traditional centralized ac power network. In terms of technological development, the applications of renewable energy and battery energy storage elements have become more mature, and more and more appliances are changed to dc power. Therefore, the development of dc microgrids (MGs) becomes the trend in future energy systems. It has already been applied in certain applications, such as marine smart ships [1], [2] and dc residential grid networks [3]–[5], and more applications will be developed in the coming future. The system architectures and the system control algorithms are two main research areas to develop dc MG technology. Apart from that, the system protection is another key concern in dc MG as it is related to the safety and stability of the whole system. Especially in the application of low-voltage (LV) public power grids, for any power generation system and solar power system fed in parallel to the grid, automatic disconnection equipment must be installed [6]–[8]. Its main purpose is to prevent any unintentional current from feeding into the subgrid or independent grid during the system shutdown. Thus, regarding the safety concern, in such applications, protection circuits with high reliability and double line physical isolation characteristics are always required.

In the past few years, due to the increasing popularity of dc MG, various hybrid protection solutions [9]–[22] have recently been proposed to provide high-quality protection features and to overcome the reliability issues of the traditional mechanical breaker solutions. The concept of hybrid solution first appears in the ac grid system. In [9], a typical ac hybrid switching scheme is proposed in which a thyristor is in parallel with the mechanical switch to interrupt the short-circuit current. As shown in Fig. 1(a), similar to [9], a typical hybrid dc circuit breaker solution is presented in [10], in which a fast mechanical switch and integrated gate control thyristor (IGCT) sets are connected in parallel. The IGCT is applied to handle the transient operation during the turn-OFF moments and to effectively improve the reliability of the circuit. However, the galvanic isolation function of the relay is disabled. An optional design is presented in [11], which is in a parallel combination of similar semiconductor devices to generate with the same functionality. In [12], a hybrid circuit breaker with a forced commutation circuit is presented, and its circuit diagram is given in Fig. 1(b). By the circuit operation, it can commutate the current to the parallel path before the mechanical circuit breaker is opened. Therefore, the total system shutdown time can be reduced, which is stayed between mechanical and solid-state solutions. However, the circuit capacitor is required to precharge, and the galvanic isolation function of the relay is disabled. Another type of hybrid circuit breaker is proposed in [13], and its circuit configuration is shown in Fig. 1(c). In the design, the main conduction path is formed by a mechanical switch and a pair of bidirectional semiconductor switches, and the alternative conduction path is

Manuscript received February 4, 2020; revised April 25, 2020 and June 29, 2020; accepted July 27, 2020. Date of publication August 3, 2020; date of current version October 30, 2020. This work was supported by a grant from Canada Research Chairs, Canada (Sponsor ID: 950-230361). Recommended for publication by Associate Editor J. M. Guerrero. *(Corresponding author: Ken King Man Siu.)*

The authors are with the Department of Electrical and Computer Engineering, RIGA Lab, University of Manitoba, Winnipeg, MB R3T 5V6, Canada (e-mail: siukm3@myumanitoba.ca; carl.ho@umanitoba.ca; lid34514@myumanitoba.ca).

Color versions of one or more of the figures in this article are available online at https://ieeexplore.ieee.org.

Digital Object Identifier 10.1109/TPEL.2020.3013612

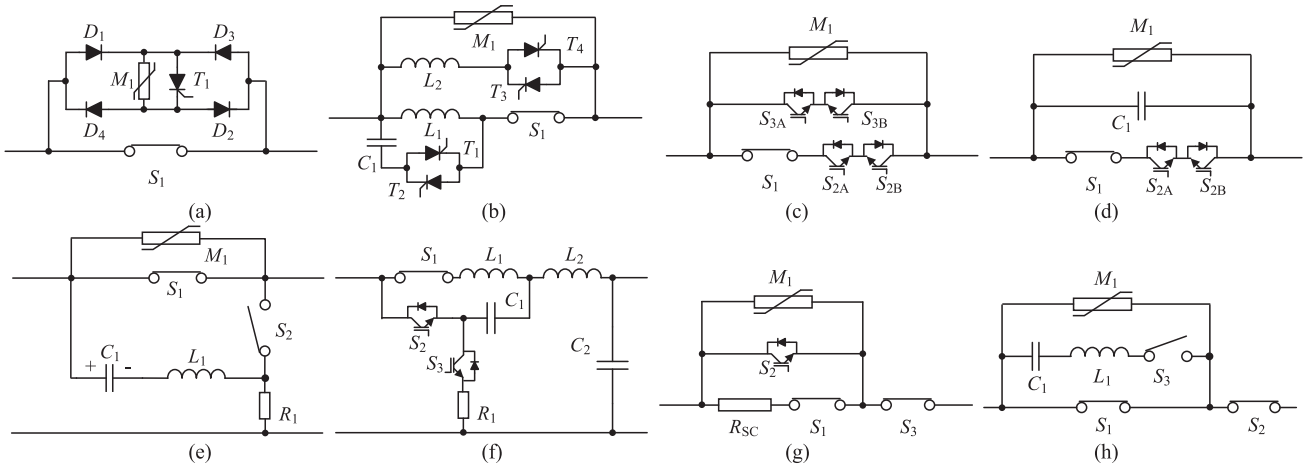


Fig. 1. Prior-arts of dc circuit breaker: (a) [10]; (b) [12]; (c) [13]; (d) [18]; (e) [19]; (f) [20]; (g) [21]; and (h) [22].

formed by another pair of bidirectional semiconductor switches. Two sets of semiconductor pairs are with different functions in the circuit, where the main path one acts as a commutation switch and the alternative path acts as the main breaker. Accordingly, compared with [10], a relatively faster short-circuit response can be obtained. However, due to the presence of two sets of semiconductor pairs in the circuit design, a higher system conduction loss is resultant and no galvanic isolation function is offered. Under the same functionality as [13], various solutions are given in [14]–[17], which are with different semiconductor combinations. In addition, in [18], an alternative solution of [13] is proposed in which the semiconductor pair in the auxiliary conduction path is replaced by a capacitor, as shown in Fig. 1(d). Therefore, the design is simplified and the number of components is reduced. However, compared to [13], the component stress in the design becomes higher and additional discharging may require the fast reclosing application. In [19] and [20], two different types of zero current switching (ZCS) hybrid circuit breaker solutions are presented, as shown in Fig. 1(e) and (f), respectively. Both are using a pre-charged capacitor to create resonant characteristics in the system during the turn-OFF transient and guide the current through the system to ensure ZCS. In [19], the reactor is connecting in series with the precharge to control resonant peak during breaking action and handle the capacitor charging action during the normal operation. The switch in the alternative conduction path can implement by a solid-state switch or other high-power switching devices. In [20], the reactor is connecting in series with the mechanical switch in the main conduction path to slow down the current flow, and two semiconductor switches are applied to control the interruption process. Both [19] and [20] have a highly efficient design; however, these ZCS solutions cannot provide galvanic isolation and bidirectional functions. To address the isolation feature, some isolated type hybrid solutions have been developed [21]–[23]. In [21], an isolated hybrid solution is presented as shown in Fig. 1(g). In the design, two mechanical switches are involved in the main current path. One is used as the main circuit switch, which will trigger immediately when a turn-OFF signal is provided, and the other is used to generate

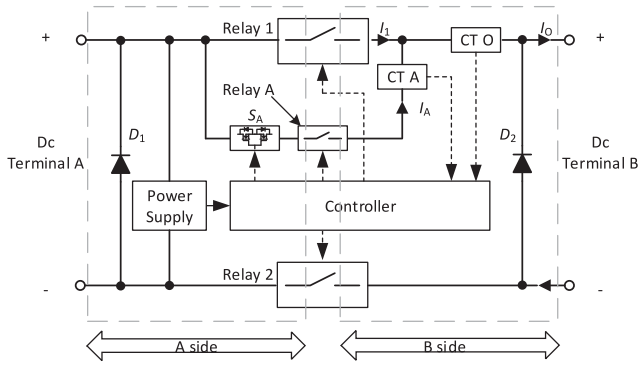


Fig. 2. Proposed dc circuit breaker.

the isolation function. Since the number of mechanical switches is twice that of traditional mechanical solutions, it will cause the conduction loss in the system to double. In [22], a ZCS type isolated hybrid circuit breaker is presented, as shown in Fig. 1(h). The switch in the alternative conduction path can be a solid-state switch or other high-power switching devices, such as spark gaps. However, similar to [21], the overall conduction loss on the positive line remains twice that of the traditional single mechanical solution. Meanwhile, with a similar feature as that of [22], another series *LC* type isolated hybrid circuit breaker is presented in [23]. Overall, a summary is given in Table I. In most cases, they have a higher probability of causing overvoltage on the switching devices. Therefore, metal oxide varistor (MOV) is always required. In addition, among those reviewed hybrid designs, they are either not supporting the galvanic isolation feature or having high conduction loss in the design but cannot achieve both at the same time.

An alternative high-reliability hybrid circuit breaker solution, as shown in Fig. 2, is proposed in this article to achieve both galvanic isolation and high-efficiency features. It is aimed at LV dc MG applications and provides low conduction loss, low device electrical stress, bidirectional current flow, and double line physical isolation feature on the entire system. In the design, each main power path is handled by a single mechanical relay to

TABLE I
SUMMARY OF NUMBER OF SEMICONDUCTOR DEVICES AND MECHANICAL COMPONENTS INVOLVED IN THE TOPOLOGIES

| Topology | Main Conduction Path | | | Auxiliary Path | | | Breaking Action in $S_1$ | Major Function | | | |
|---|---|---|---|---|---|---|---|---|---|---|---|
| | Switch | | Passive Device | Switch | | Passive Device | | Bidirectional | Durability | Galvanic Isolation | Possibility of Overvoltage |
| | Type | Total Cond. | | Type | Total Cond. | | | | | | |
| Fig. 1a | 1 Mech. | 1 | 0 | 5 Semi. | 3 | 0 | LV Turn-off | Yes | High | No | High |
| Fig. 1b | 1 Mech. | 1 | 1 | 4 Semi. | 1 | 2 | ZCS | Yes | High | No | High |
| Fig. 1c | 1 Mech. + 2 Semi. | 3 | 0 | 2 Semi. | 2 | 0 | ZCS | Yes | High | No | High |
| Fig. 1d | 1 Mech. + 2 Semi. | 3 | 0 | 0 | 0 | 1 | ZCS | Yes | High | No | High |
| Fig. 1e | 1 Mech. | 1 | 0 | 1 Power Switch | 1 | 3 | ZCS | No | High | No | Middle |
| Fig. 1f | 1 Mech. | 1 | 2 | 1 Semi. | 2 | 1 | ZCS | No | High | No | Low |
| Fig. 1g | 2 Mech. | 2 | 1 | 1 Semi. | 1 | 0 | LC Turn-off | No | High | Yes | High |
| Fig. 1h | 2 Mech. | 2 | 0 | 1 Power Switch | 1 | 2 | ZCS | No | High | Yes | Middle |
| Fig. 2 (proposed) | 1 Mech. | 1 | 0 | 1 Mech. + 2 Semi. | 2 | 0 | LV Turn-off | Yes | High | Yes | Low |

produce a low-resistance connection path and physical isolation during the turn-ON and turn-OFF periods, respectively. A mixed switch auxiliary path is given in the hybrid solution to separately handle the transient process. Thus, a smooth current exchange between the main conduction path and the auxiliary conduction path is realized and the electrical stress in the mechanical relay is minimized. Therefore, the durability of the mechanical relay is enhanced, and it provides the possibility of using an ac relay in a dc circuit. Meanwhile, by combining the characteristics of protection diodes and auxiliary path, the proposed circuit has the surge current capability, and the possibility of overvoltage is highly reduced. Therefore, the overall solution is with high reliability and high efficiency. The operation principles of the presented solution and the design guideline are given in this article. Targeting LV dc MGs, a 150/380 V and 15 A experimental prototype has been implemented to verify the operation of the proposed circuit. The experimental results and detailed findings were consistent with the theoretical analysis.

## II. PRINCIPLE OF OPERATION

### A. Circuit Structure

The proposed solution consists of two main conduction paths and an auxiliary conduction path, where the main paths are composed of two main power relays, Relays 1 and 2, and the auxiliary path is formed by a pair of semiconductor devices $S_{\mathrm{A}}$ and a series auxiliary relay Relay A. Meanwhile, two identical diodes, $D_1$ and $D_2$, are included in each terminal end for the protection purposes. Two sets of current sensors, $CT_{\mathrm{A}}$ and $CT_{\mathrm{O}}$, are applied to measure the power line current and the auxiliary line current as $i_{\mathrm{O}}$ and $i_{\mathrm{A}}$ separately. The details of the configuration are shown in Fig. 2.

Among those three mechanical relays, two of them are used to provide isolation on the main conduction path and the third one provides isolation in the auxiliary conduction path. As a result, when a fault appears, both sides of the breaker circuit system can be physically isolated and a safe system environment can be guaranteed in the targeting MG application. Relays 1 and 2 are the two main relays in the circuit, which are used to establish the connection path between two system ends for the normal operation. Relay A is the auxiliary relay in the circuit, which is used to establish the connection path for the semiconductor pair and acts as the major conduction channel during the transient process. Both Relay 2 and Relay A operate at ZCS, and Relay 1 always switches with a parallel conduction channel. Therefore, component stress faced at the switching transients can be significantly reduced.

The pair of semiconductor devices only functions actively during the turn-ON and turn-OFF transient periods and acts as a main breaker of the whole system. The semiconductors are used to compensate for the energy during breaking action instead of using mechanical relays. As a result, the durability of the mechanical breaker system is enhanced and a fast breaker action can be achieved in any current or loading conditions. Thus, the proposed solution is with high system reliability. It can be realized by connecting two MOSFETs back-to-back in series connection or other bidirectional blocking switch configurations.

The pair of diodes may only function actively during the OFF transient and act as protective devices in the circuit to avoid any overvoltage conditions caused by the induced energy. Therefore, different from other hybrid solutions [10], [12], [18] in the proposed solution, the semiconductor pairs will not reach the overvoltage value. The resultant electrical stress in the components is less than others, and a parallel MOV is not required in the design. In order to realize the bidirectional protection function in the designed system, it is necessary to place an identical diode on each terminal.

In order to achieve a smooth current transient in the mechanical relays, a specific operation sequence is required. The accurate fault detection and a correct switching pattern are produced from the sensing information. According to the operating situations, the dc breaker will operate in different scenarios. A detailed operational sequence at the normal situations is given in Figs. 3 and 4, respectively. Also, a program flow of the turn-OFF sequence is given in Fig. 5.

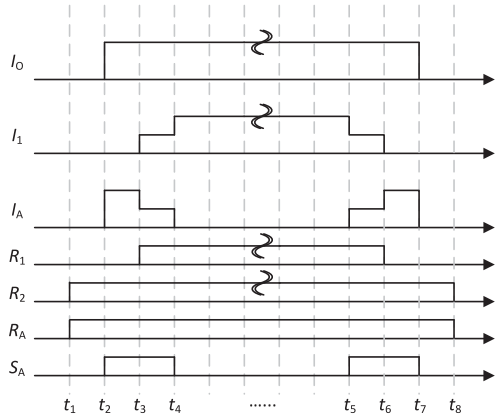


Fig. 3. Operation sequence of the proposed dc circuit breaker.

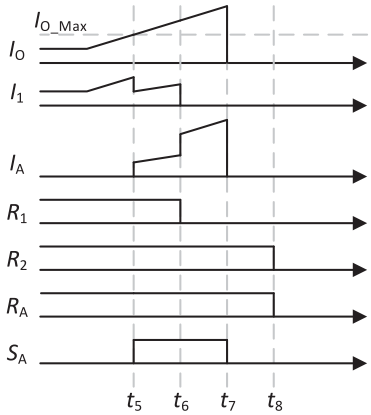


Fig. 4. Operation sequence during fault detection.

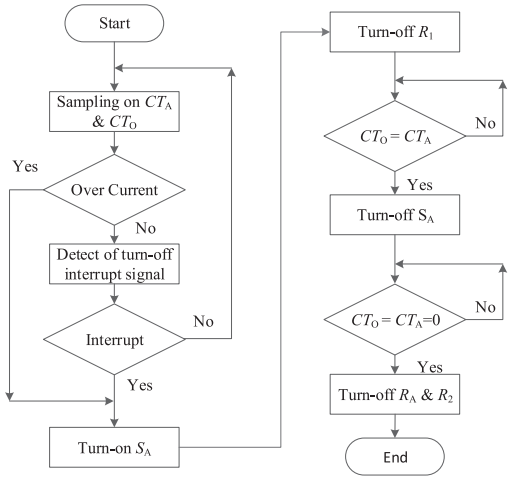


Fig. 5. Program flow in turn-OFF sequence.

### B. Operation Sequence at Turn-ON Situation

*Stage 1 ($t = t_1$):* After the start-up signal is given, the circuit begins to operate. Turn-ON signals are given to $R_2$ and $R_A$. During this time, $R_2$ becomes ON and provides a return path for current. At the same time, the physical isolation of the auxiliary path is removed. $R_A$ becomes conduction and establishes a path to connect semiconductor devices to both system terminals. At this period, the main conduction path is not yet established; so no current flows through the circuit. This stage accomplishes when $R_2$ and $R_A$ are fully conducted.

*Stage 2 ($t = t_2$):* A turn-ON signal is given to $S_A$ to release the bidirectional blocking from the semiconductor devices. During this time, $S_A$ becomes ON and a connection path between both ends of the circuit is established as an auxiliary channel. The dc current starts to flow from one terminal to the other through the auxiliary path as $I_A$. This period ends after the semiconductor is fully ON.

*Stage 3 ($t = t_3$):* A turn-ON signal is given to $R_1$. During this time, $R_1$ becomes ON. Due to the presence of the auxiliary path, $R_1$ can switch under a relatively LV condition and within the ac relay specified dc switching voltage. The major connection path between both positive terminals is built up. Due to the lower resistance characteristic, the dc current will bypass the auxiliary path and start to flow through $R_1$ as $I_1$. The overall output current $I_O$ remains the same at the last stage; however, $I_A$ is reduced. This period will end after $R_1$ is fully ON at a certain time and a current reduction in $I_A$ is detected.

*Stage 4 ($t = t_4$):* A turn-OFF signal is given to $S_A$ to disable the auxiliary conduction path. During this time, $S_A$ becomes OFF and switches under a relatively LV condition. Afterward, the auxiliary channel is electrically disconnected from the main circuit. The dc current will only flow through the main relays, in which $I_1$ becomes the same as $I_O$. This period ends when $I_1$ becomes zero. And the system turn-ON transient sequence is finished and only two main relays are remaining ON.

### C. Operation Sequence at Turn-OFF Situation

*Stage 5 ($t = t_5$):* After a disconnection signal is given from the general shutdown operation or the fault detection, the circuit turn-OFF operation sequence begins. A turn-ON signal is given to $S_A$ to set up an auxiliary conduction path for the power flow, and the current conduction behavior will be the same as that in stage 3. This period will end after the semiconductor is fully ON and a current reduction in $I_1$ is detected.

*Stage 6 ($t = t_6$):* A turn-OFF signal is given to $R_1$. During this time, $R_1$ becomes OFF. Due to the presence of the auxiliary path, $R_1$ can switch under a relatively LV condition and within the ac relay specified dc switching voltage. The main conduction path in the positive terminal is disconnected; thus, $I_1$ is forced to zero. The circuit remains conducting and the situation is the same as that in stage 2. This period ends after $R_1$ is fully OFF and the current value of $I_A$ is exactly equal to $I_1$.

*Stage 7 ($t = t_7$):* A turn-OFF signal is given to $S_A$ to disable the auxiliary conduction path. During this time, $S_A$ becomes OFF, and it acts as the main breaker during this period. All energy among the breaking action will be dissipated through the semiconductor devices. Therefore, the selection of the semiconductor is very significant in the design. This period ends when $I_1$ becomes zero and the bidirectional blocking feature is reformulated. No more current is flowing through the breaker circuit.

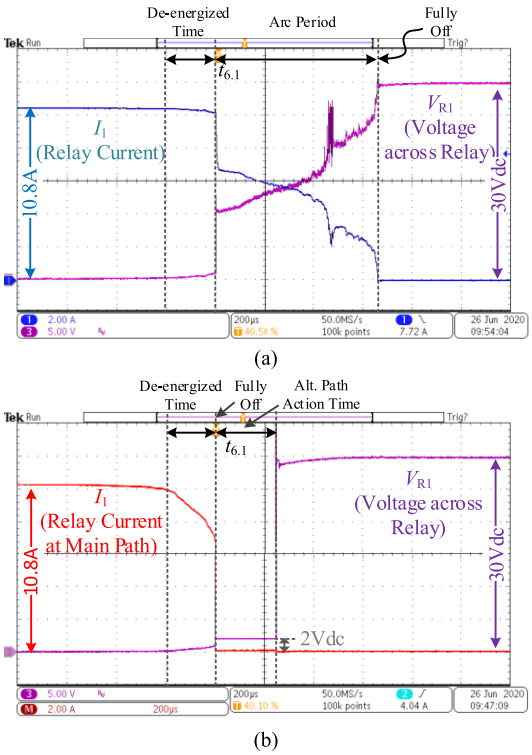


Fig. 6. Breaking waveforms of (a) traditional mechanical solution and (b) proposed breaker solution.

*Stage 8 ($t = t_8$):* A turn-OFF signal is given to both $R_A$ and $R_2$. During this time, both relays become OFF and switch under ZCS operation. At the turn-OFF transient, no electrical stress is applied to the device. Afterward, both of the auxiliary and the current return paths are physically disconnected from the main circuit. As a result, through the dc circuit breaker, both sides of the systems are fully isolated from each other. This can guarantee to have a safe environment for workers during grid or device repairing. The circuit remains OFF until a reconnection signal is given.

### D. Arc Characteristic During Breaking

The major difference between the traditional mechanical solution and the proposed hybrid solution is on the arc handling. A set of electric performance comparisons is given in Fig. 6(a) and (b) to demonstrate the difference between both solutions.

In the traditional mechanical solution, as shown in Fig. 6(a), when the opening signal is provided to the circuit breaker, the coil energy will start to be eliminated, which causes the contacting plane to be separated and restored to its original position. Afterward, the contacting plane will begin to separate and the contacting area will be reduced, which leads to an increase in both contacting resistance and current density on the contacting plane at the same time. Thus, the pressure between the contacts decreases and the temperature increases. At $t_{6.1}$, the contact planes are separated. In the case of low pressure and high temperature, the air in between will be ionized, thereby creating a low-resistance path for the main current to pass through: that is the arc we can observe [25], [26]. The intensity and duration of the arc mainly depend on the voltage stress and current magnitude. The energy dissipated during the mechanical breaking action can also be estimated based on the total cross-sectional area in the electrical waveform. When the contact returns to its original position and has high-resistance insulation, the circuit breaker will completely open again.

TABLE II
CIRCUIT BREAKER PERFORMANCE COMPARISON ON A 30 VDC AND 10.8A SYSTEM

| Solution | Energy Dissipation | Duration |
|---|---|---|
| Mechanical Fig.6 (a) | 45.82 mJ | 660 µs |
| Proposed Fig.6 (b) | 167.3 µJ | 140 ns |

In the proposed hybrid solution, the de-energized process is similar to the traditional solution. However, due to the existence of the auxiliary conduction path, when the contacting area begins to decrease, only the contacting resistance will increase, but the current density on the contacting plane will not be affected. It is also proved in Fig. 6(b) that since the contacting resistance keeps increasing at the separation period, a significant current reduction is observed. At $t_{6.1}$, the contact planes begin to separate, the dc current will be immediately transferred from the main conduction path to the auxiliary conduction path, and the transient process will be completed in a very short period of time under a relatively LV condition. In Fig. 6(b), it clearly demonstrates the benefit of the proposed method, in which the energy dissipation during the turn-OFF transient is reduced to $\mu$J range and is 274 times lower than the traditional solution. A detailed summary is given in Table II. In most cases, because the energy dissipated in the mechanical switches is limited in a small amount of value, the contacts will no longer rise to a high temperature value at the transient action and the ionization will not occur. In the meantime, according to Fig. 6, the corresponding resistivity over time and the switching trajectories at the turn-OFF transient are found and are given in Fig. 7(a) and (b), respectively. It clearly showed that no ionized low conduction path had resulted, and the main relay was able to turn-OFF in a relative LV range. Thus, the possibility of arcing is highly reduced and a smooth reopening is able to provide in each mechanical switching action. By having an appropriate circuit design, the energy dissipated in the mechanical switch can be limited to a specific value that does not cause ionization and arcing. Even in some unexpected situations, the energy is higher than expected, and the mechanical relay still has the ability to handle the arc at the specified power rated of the relay and will not cause any system failure. A detailed switching diagram on the positive terminal is also given in Fig. 8 to explain the current flow during the turn-OFF transient.

## III. SELECTION OF COMPONENTS

The proposed circuit is a hybrid dc breaker solution, which consists of both mechanical relays and semiconductor devices. In a traditional dc breaker solution, a single mechanical relay or a solid-state breaker is applied to act as both power line

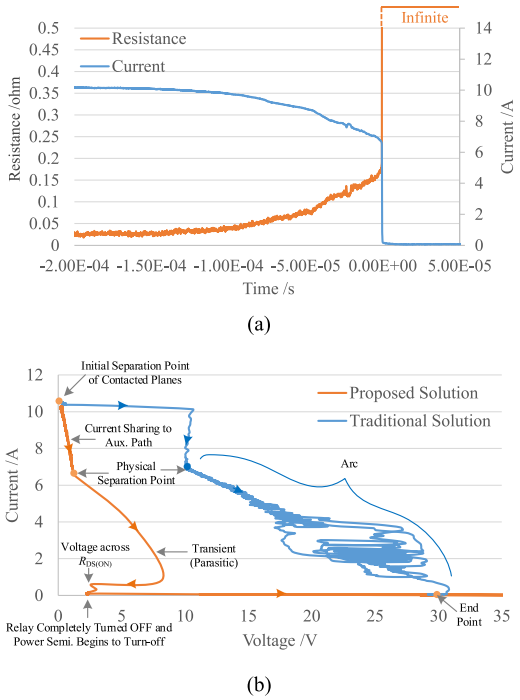


Fig. 7. Main relay performance diagram. (a) Resistance change with time. (b) Switching trajectories during stage 6.

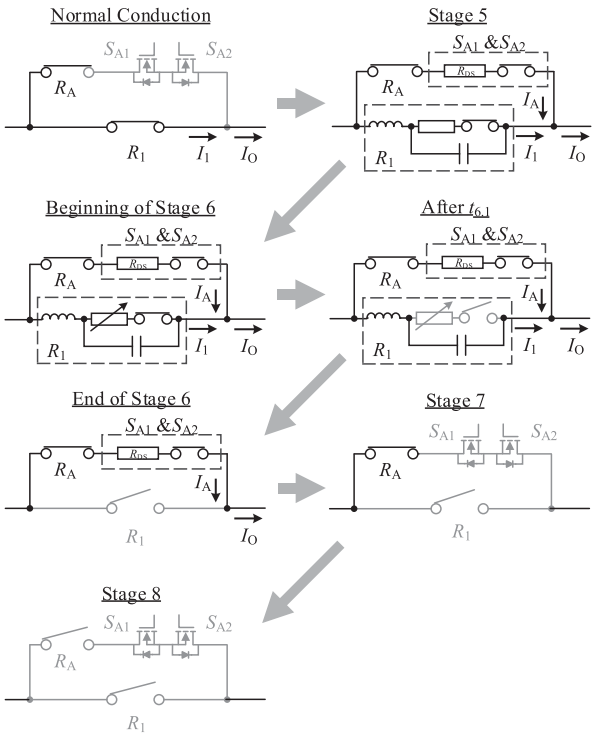


Fig. 8. Equivalent circuit on positive terminal during turn-OFF transient.

current conductors during the normal situation and circuit breaker during the transient situation.

Among the traditional breaker technologies, mechanical relay and solid-state relay are two of the commonly used devices. Some of the existing dc breakers on the markets are listed in Table III as reference. The key features are highlighted in the table. The mechanical relays are physical switches, which use the electromagnetic contact to control the circuit operation. They are with low-conduction resistance and can provide high-level insulation on the device. However, it is not able to handle the surge current and the durability is usually poor, around 10 000 times. In contrast, the solid-state relays are most likely semiconductor-based. It provides fast response and low contacting arc. The drawback is the high conduction resistance and the absence of physical isolation. Hence, for solid-state relays, the overall system reliability is limited and the system efficiency is restricted.

Different from the single breaker solution, in the proposed solution, the major functions in the dc breaker circuit solution are separated clearly into two divisions, current conduction and circuit breaking. Each function is handled by a certain device; the advantage of both types of device can be fully utilized, while their disadvantages are eliminated in the hybrid solution. In the design, mechanical relays are selected to handle the current conduction in the power line during the normal situation, and semiconductor switches are selected to handle the breaking action during the transient period. The target system parameters are highlighted in Table III.

### A. *Selection of Mechanical Relays*

In the traditional approach, during each switching action, an electrical arc will be generated between the two contacted planes. One of the examples is given in Fig. 9(a), which is conducted under the on-site test. Under high-voltage and high-current ON–OFF actions, the resulting high energy electrical arc will heat the contacted plane and oxidize a small portion of the surface each time. The oxidized area will become high resistance and affect the system performance in the next braking action. After a long-term repetitive breaking action, the surface will be completely oxidized and the contactor may be bent, as shown in Fig. 9(b). As a result, the relay will no longer function properly and result in failure.

In the proposed solution, mechanical relays are applied to handle the current conduction in the power line during the normal situation and to provide a physical isolation feature. Thus, when selecting, both voltage and current ratings are important parameters to be considered. The voltage rating of the relay is used to support the breakdown voltage of the system, and the current rating of the relay is used to handle the current capability during the conduction period. Meanwhile, response time is another parameter in concern. In the proposed solution, it targets for LV public grid application. Thus, it is required that the selected relay has a response time of milliseconds.

As discussed in Section II, different from the traditional approach, in the proposed solution, all the mechanical relays are switched under low energy dissipation conditions. Therefore, in the proposed solution, the choice of relays becomes more extensive, and the design can consider the following.

1) *The use of ac relays in a dc relay circuit:* All the relays are switched under either relatively LV or floating conditions, which means that the electrical stress applied to the components during the transient actions is at a relatively

TABLE III
SYSTEM PARAMETER COMPARISON WITH COMMERCIAL PRODUCTS

| Model | Hongfa -HFS33/D-200D10M | Crydom -84137850 | TE Connectivity -AP10B245 | Omron Electronics -G9EB-1 | Proposed |
|---|---|---|---|---|---|
| Type | SolidState | SolidState | Mechanical Vacuum Relay | Mechanical with gas-filled | Hybrid |
| DC Voltage /V | 200 | 200 | 270 | 250 | 380 |
| DC Current /A | 10 | 10 | 10 | 20 | 15 |
| Max Surge /A (10ms) | 40 | 60 | N/A | N/A | 80 |
| Resistance / Ω | 105m | 210m | 10m | 30m | < 5m |
| Electrical Durability | > 100k | > 100k | 7k | 30k | > 100k |
| Dielectric Strength | N/A | N/A | 2000 Vrms | 2500 Vrms | 1000 Vrms |


(a) (b)

Fig. 9. Experimental diagrams of mechanical relay (a) during electric arcs and (b) after repetitive switching action.

low value and can be limited within the ac relay specified dc switching voltage. The ac voltage rating of the relays is only used to guarantee that the circuit is with enough voltage insulation for the system. Therefore, ac relays can be adopted into the selection on the mechanical relays instead of the bulky and expensive dc relays. For example, a 250-Vac relay can apply to a dc circuit breaker design up to 353.6 Vdc. Therefore, it is especially suitable for LV dc MG.

2) *Mechanical durability as relay durability instead of using electrical durability:* The main power relay $R_1$ is always paralleled with a low-resistance path during the switching transient. Thus, a smooth current transient is always guaranteed in $R_1$. The other two relays, $R_A$ and $R_2$, are even better which are switched under zero current situation. All the relays are switched with low energy dissipation and the possibility of the electrical arc becomes relatively small. Accordingly, it provides an opportunity to extend the electrical durability of the applied mechanical relays to a value close to the mechanical durability defined in the datasheet and result in a longer life time in the entire solution compared to the traditional fully mechanical solution. The extension of life time will be more dependent on the maximum amount of energy dissipation in the mechanical relays.

Overall, in the target 150/380 Vdc and 15 A dc breaker system, an ac relay, G2R-1A-E, is selected. It features with a 16-A current capability, a maximum 380-Vac switching voltage, 100 000 times in mechanical durability, 2-mΩ low-resistance characteristic, and 7–9 ms mechanical action time. Thus, it fits for the target power ratings and helps to produce designs with high durability and high efficiency.

### B. Selection of Semiconductors

In the design, semiconductor switches are applied to handle the transient switching action in the breaker circuit. A pair of semiconductor switches is required to apply at the same time to produce the bidirectional blocking characteristic. For discrete devices, they can be arranged into a back-to-back, drain-to-drain, or other bidirectional configuration. In the selection, the voltage and current ratings of the semiconductors are determined by the operating voltage and the current capability of the system, respectively. In addition, inrush current capability is another parameter to consider in semiconductor selection. It is used to support the system response during faults and is defined by the maximum short-circuit current and the worst-case energy information in the system.

Among the switching sequences, the most critical breaking action appears in stage 7. At stage 4 and stage 5, $S_A$ is switched ON and OFF under relatively LV conditions, respectively. However, at stage 7, due to the presence of parasitic inductance in the loop, high voltage stress will occur between the drain and source of the semiconductor under the turn-OFF transient. The detailed switching action of $S_A$ during stage 7 is given in Fig. 10.

A pair of protection diodes has been applied to the system and, generally, no overvoltage conditions will occur. However, for IGBTs or other semiconductor devices without overvoltage capability, a parallel MOV is still recommended to avoid any excessive transient voltages. Differently, power MOSFET does

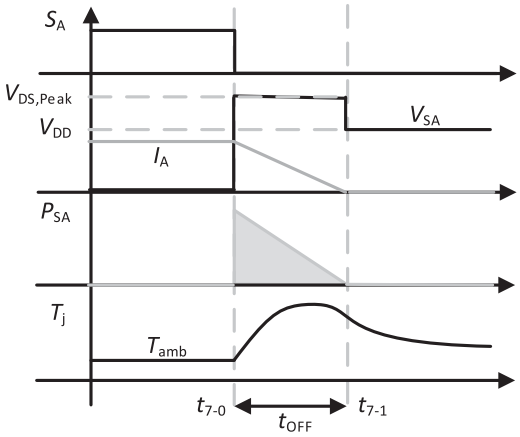


Fig. 10. MOSFET overvoltage performance at stage 7.

not have this requirement. Inside a traditional MOSFET, there is a group of parasitic components inside the physical structure, such as parasitic resistance in P-well channel structure and a parasitic n-p-n bipolar transistor structure [27]. Normally, the parasitic n-p-n is effectively shorted. However, during the turn-OFF moment, a strong electric field is resultant inside the device which causes current flow proximity to the parasitic n-p-n transistor internally. Once sufficient voltage is generated on the parasitic bipolar transistor, it will be activated, and will claim the device voltage at a value that is 1.2–1.3 times higher than the general breakdown voltage. Thus, the avalanche characteristic can protect the power MOSFET from overvoltage, which makes it more suitable for LV MG applications.

The worst-case energy is able to determine from the circuit relationship at stage 7. By applying Kirchhoff's voltage law to the main current loop, the detail characteristic of the overvoltage or the avalanche period can be determined. The circuit relationship at stage 7 is formed as

$$V_{\mathrm{DD}} = V_{\mathrm{DS,Peak}} + L_{\mathrm{loop}} \cdot \frac{dI\,(t)}{dt} + R_{\mathrm{loop}} \cdot I\,(t) \qquad (1)$$

where $V_{\mathrm{DD}}$ is dc voltage at the input side, $V_{\mathrm{DS,Peak}}$ is overvoltage or the avalanche voltage applied to the semiconductor in stage 7, $I$ is dc current flowing in the circuit, $L_{\mathrm{loop}}$ is loop inductance or parasitic inductance in the current path, and $R_{\mathrm{loop}}$ is parasitic resistance at the current path.

By solving (1) with the start point and the endpoint circuit information, the corresponding turn-OFF time $t_{\mathrm{OFF}}$ is determined as

$$t_{\mathrm{OFF}} = \frac{L_{\mathrm{loop}}}{R_{\mathrm{loop}}} \ln\left[1 + \frac{I_{\mathrm{peak}} \cdot R_{\mathrm{loop}}}{V_{\mathrm{DS,Peak}} - V_{\mathrm{DD}}}\right]. \qquad (2)$$

During the turn-OFF period, the power dissipation in the MOSFET is approximating to a triangle waveform. Accordingly, the corresponding energy dissipation $E_{\mathrm{OFF}}$ is simplified to

$$E_{\mathrm{OFF}} \cong \frac{1}{2} \cdot V_{\mathrm{DS,Peak}} \cdot I_{\mathrm{peak}} \cdot \frac{L_{\mathrm{loop}}}{R_{\mathrm{loop}}} \ln\left[1 + \frac{I_{\mathrm{peak}} \cdot R_{\mathrm{loop}}}{V_{\mathrm{DS,Peak}} - V_{\mathrm{DD}}}\right]. \qquad (3)$$

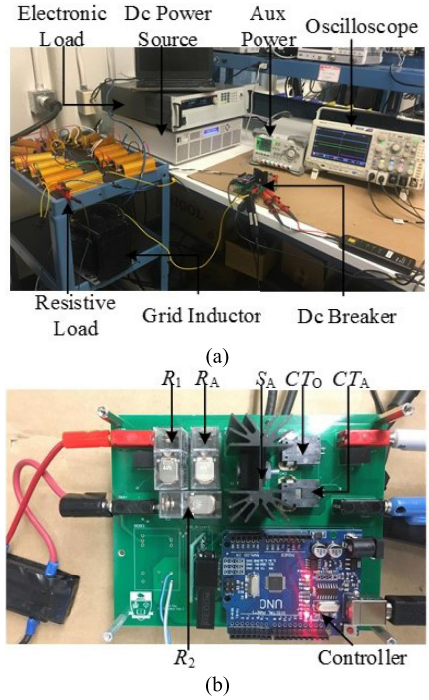


Fig. 11. Hardware diagrams of (a) test setup and (b) dc circuit breaker prototype.

With the use of (3), the maximum rating in the target system, and a 2-$\mu$H parasitic loop inductance as the worst-case assumption, a 0.2-mJ worst-case energy dissipation can be calculated.

According to the maximum rating of the target system, 150/380 Vdc and 15 A, the worst-case energy dissipation, 0.2 mJ, and a five-time short-circuit capability, 75 A, in the target dc breaker system, a discrete TO247 power MOSFET, IPW60R125C6, is selected. It features with a 0.96-mJ for repetitive energy, around 89-A pulse current at 25 °C, and with a 600 Vdc breakdown. A summary of the selected components is given in Table IV.

## IV. Experimental Verifications

A 150/380 Vdc and 15 A test platform with a dc breaker prototype, as shown in Fig. 11, is built to verify the performance of the proposed dc circuit breaker and the target operating conditions defined in Table I. The prototype shows that the entire system is controlled by a single microcontroller and the protection feature comes from the accurate current detection by the Hall-effect sensors. Compared to the two-relay traditional system, in the proposed solution, an extra relay and a pair of semiconductor switches were applied, in which the semiconductor pair was arranged in back-to-back connection. According to the given control strategy, the power consumption of the auxiliary circuit was kept within 3 W. At the standby mode, only 0.95 W was consumed. At the normal operation mode, 2.85 W was consumed, which is closed to the traditional approach.

In Fig. 12, it demonstrates a complete operating sequence of the proposed circuit during ON and OFF conditions under a 10-$\Omega$ resistive load and 150-Vdc input. The resultant operational

TABLE IV
SELECTED COMPONENTS IN THE PROTOTYPE

| Device | Requirement | | | Selection | |
|---|---|---|---|---|---|
| | Conduction | Isolation | Switching | Model | Type |
| $R_1$ | Power Line | Yes | Low Voltage | G2R-1A-E | AC Mechanical Relay |
| $R_2$ | Power Line | Yes | ZCS | G2R-1A-E | AC Mechanical Relay |
| $R_A$ | Auxiliary Path | Yes | ZCS | G2R-1A-E | AC Mechanical Relay |
| $S_A$ | Auxiliary Path | No | None | IPW60R125C6 | MOSFET |

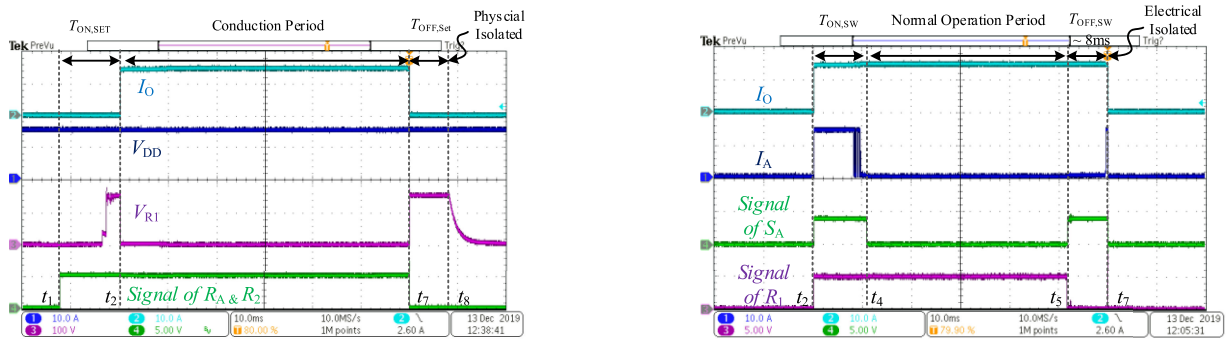


Fig. 12. Experimental results under purely resistive loading that relates to (a) circuit isolation feature and (b) current conduction channel.

sequence was the same as the one proposed in Section II. In each transient operation, it was able to divide into two parts: The electrical operation process, $T_{ON,SW}$ and $T_{OFF,SW}$, and the physical setting process, $T_{ON,SET}$ and $T_{OFF,SET}$. In both actions, their durations are also highly dependent on the response time of mechanical relays, which are about 7–9 ms. For example, in Fig. 12(a), after the turn-ON signal provides $R_1$ at $t_1$, it takes 8 ms to settle, and then the semiconductors respond in another few hundred ns and complete the electrical operation process. A similar situation appeared in the physical setting process. Overall, the electrical transient action was able to complete in 8 ms, which fulfills with requirement protection feature in dc MGs of fault current interruption within 0.01 s [28], [29] and is compatible with other mechanical-based LV dc hybrid circuit breaker solutions and mechanical solutions in ms response time [20], [29]. Together with the physical isolation action, the overall required start-up time was around 23 ms and the overall turn-OFF action was within 16 ms. The slight difference in the switching transient time comes from the charging and discharging characteristic of $R_A$. In the turn-ON period, the energy comes from an auxiliary power; thus, the maximum supplying power is limited and it causes a longer time to charge. In the turn-ON period, the energy comes from an auxiliary power, and, thus, the coil power is released through a freewheeling diode and a compensation resistor; thus, a fast discharging time is resultant.

In Fig. 12(a), it shows the switching pattern that relates to the physical setting process, where $R_2$ and $R_A$ are synchronized in action. During this processing period, the system did not have any power flow and operated at ZCS. It either worked to establish a system connection path at $t_1$ before the current flow began or to produce the physical isolation at $t_8$ after the current return path was disconnected. In Fig. 12(b), it shows the switching pattern that relates to the electrical operation process. $S_A$ was only active during the switching transient at the dc breaker circuit. It provided an auxiliary path for the current conduction during the transient period. $R_1$ was only switched when $S_A$ was active. Thus, it always operated with a parallel auxiliary path during the ON–OFF action. A smoothly current transient waveform was observed in waveform and no electrical arc was visually observed from the experimental setup.

Under the purely resistive loading, the turn-ON and turn-OFF switching performances of the semiconductor pair at the 150-Vdc system are shown in Fig. 13(a) and (b), respectively. In both cases, the switching time was also maintained within 1 $\mu$s. It proved that the major restriction in the operation time of the hybrid circuit was mainly limited by the mechanical operation. If a faster system response is required, an ultra-fast mechanical ac relay can be considered in $R_1$ and the rest of the circuit does not affect. But there is a tradeoff of cost and response time. Also, from Fig. 13, it demonstrates that the semiconductor pair is able to handle the transient responses in the dc breaker circuit properly and no overvoltage scenario happens. Thus, a safe response was still able to be guaranteed.

For the designed platform, the maximum safety voltage capability is 380 Vdc. Under this condition, a stable performance is able to be guaranteed and is demonstrated in Fig. 14. In Fig. 14(a), it shows a complete operating cycle of the proposed solution at 380-Vdc operating voltage, where the operation remains the same as in the 150-Vdc test case. Also, as shown in Fig. 14(b), a fast semiconductor action is provided by $S_A$ and no

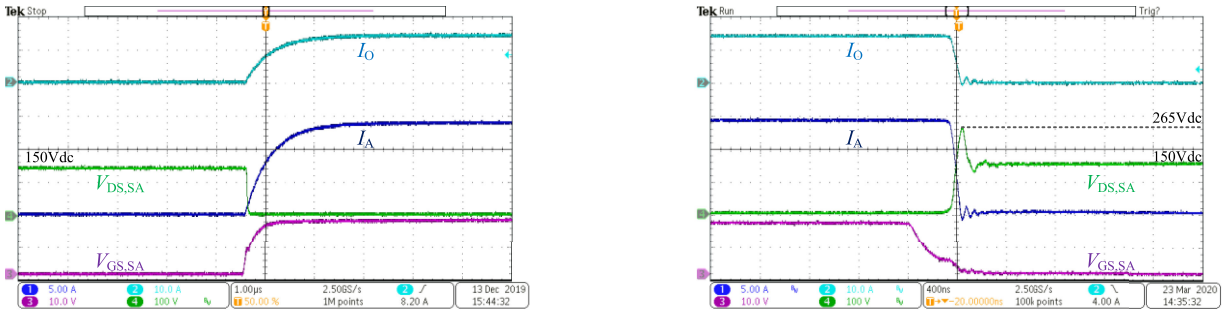


(a) (b)

Fig. 13. Experimental results of $S_A$ under purely resistive loading at 150 Vdc 15 A system. (a) Turn-ON transient at $t_2$. (b) Turn-OFF transient at $t_7$.

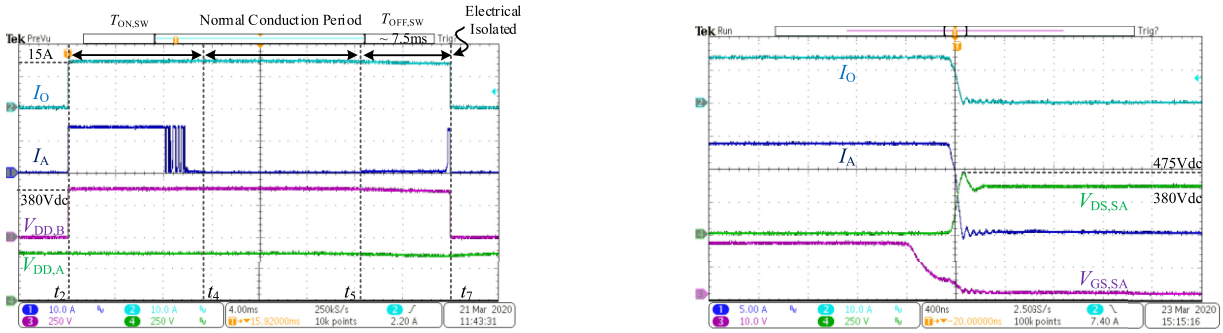


(a) (b)

Fig. 14. Experimental results under purely resistive load at 380 Vdc 15 A system. (a) Full cycle switching performance. (b) Turn-OFF transient of $S_A$ at $t_7$.

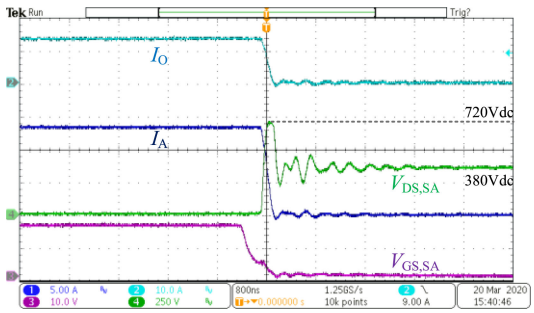


Fig. 15. Turn-OFF transient result of $S_A$ without diode protection situation.

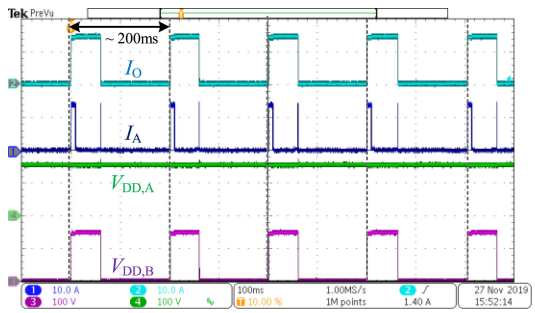


Fig. 16. Reliability testing sequence under pure resistive load.

overvoltage scenario happens. Overall, the electrical operation time is maintained within 8 ms and no electrical arc is visually observed.

In Fig. 15, the platform serves with the same working condition as Fig. 14, where the only difference was the protection diode being eliminated in the test. Even though a purely resistive load is connected, due to the presence of circuit parasitic inductance, the semiconductor is still easy to be overvoltage at the turn-off transient. A high electrical stress is induced to the semiconductor device. Thus, it was important to have the protection diode in the design to avoid the occurrence of overvoltage.

In order to verify the reliability and the bidirectional capability of the platform, a group of performance test has been done and is shown in Figs. 16 and 17, respectively. In Fig. 16,

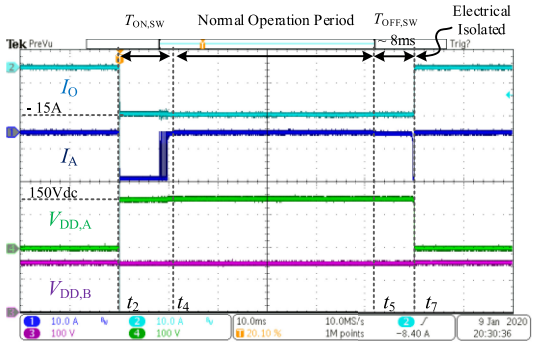


Fig. 17. Experimental result under reverse current flow.

repeated interrupts are performed on the designed system. The test sequence is given with 200 ms per cycle at 150 Vdc and

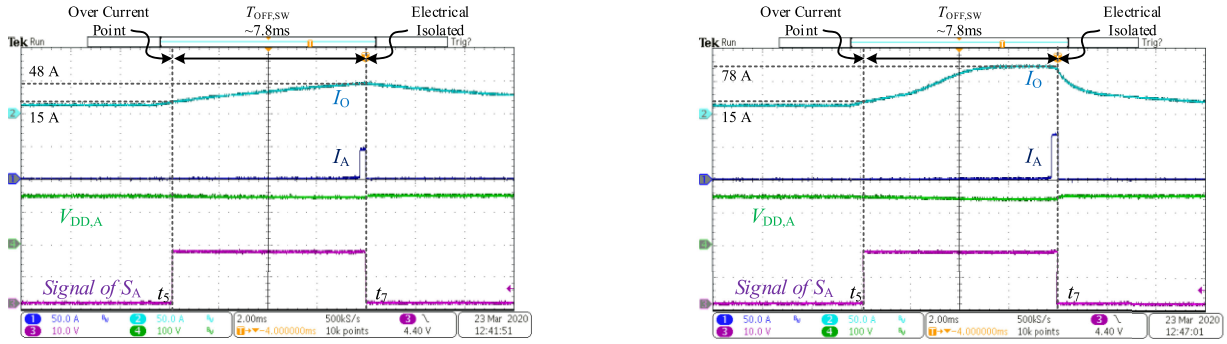


Fig. 18. Experimental results of overcurrent protection under inductive load: (a) Breaking at 48 and (b) 78 A.

15 A. Two sets of circuit prototypes were tested. Both of them were capable of running cycles above 100 thousand times, which was much higher than the traditional mechanical solution shown in Table III. Thus, the high durability performance of the proposed solution is experimentally verified. In Fig. 17, a reverse conduction situation is demonstrated, in which the current direction is opposite to the test result in Fig. 12. Under the same circuit settings, it shows the same performance in both current directions. Thus, it proved that the system was able to achieve stable performance in bidirectional current flow.

Apart from the normal shutdown operation, the system also had a stable performance under fault scenarios. In Fig. 18, it demonstrates the system performance at an overcurrent scenario. In the evaluation, an inductive load was applied, which was formed by a 20-mH grid inductor and a 12.5-Ω electronic load. To perform the overcurrent assessment, load transient was applied to result in an over-specified current to appear and the system would trigger when the current exceeded the limit of 15 A. In Fig. 18(a), the output load was dropped from 12.5 to 3 Ω and the system successfully disconnects both terminal connections at an overrating current of 48 A. Similarly, in Fig. 18(b), the output load was dropped from 12.5 to 1.67 Ω, and the system successfully disconnects both terminal connections at an overrating current of 78 A. In both cases, the electrical switching time was maintained within 8 ms, low energy dissipation in all those relays, no electrical arcs were visually observed, and a correct semiconductor breaking waveform was observed. Meanwhile, the inductive energy was handled well by the protection diode after the circuit breaker was opened. All the performance was kept the same as the normal operation. Overall, a stable protection system was guaranteed.

## V. Conclusion

This article presented an alternative solution to the dc breaker design. In the concept, it makes use of both mechanical switches and semiconductor switches. Each of them deals with a key feature in the dc breaker. The mechanical switches focus on the normal conduction, and the semiconductor switches handle the breaker transient. Therefore, the breaker design guarantees bidirectional current flow, galvanic isolation, high reliability, and high efficiency for LV dc applications. The performance of the proposed concept was experimentally verified in a 250-V, 15-A dc breaker setup, where the operation of both resistive and inductive loads has been tested. The results showed that the proposed solution achieved a fast response in switching action and was featured with high-reliability performance. All the demonstration results showed a good agreement between theoretical concepts and experimental results. The proposed dc hybrid breaker is promising for the applications of LV dc grid, photovoltaic (PV) array, and battery protection.

## References

[1] A. Accetta and M. Pucci, "Energy management system in DC micro-grids of smart ships: Main gen-set fuel consumption minimization and fault compensation," *IEEE Trans. Ind. Appl.*, vol. 55, no. 3, pp. 3097–3113, May/Jun. 2019.

[2] Z. Jin, L. Meng, J. M. Guerrero, and R. Han, "Hierarchical control design for a shipboard power system with DC distribution and energy storage aboard future more-electric ships," *IEEE Trans. Ind. Inform.*, vol. 14, no. 2, pp. 703–714, Feb. 2018.

[3] P. Sanjeev, N. P. Padhy, and P. Agarwal, "Peak energy management using renewable integrated DC microgrid," *IEEE Trans. Smart Grid*, vol. 9, no. 5, pp. 4906–4917, Sep. 2018.

[4] L. Roggia, L. Schuch, J. E. Baggio, C. Rech, and J. R. Pinheiro, "Integrated full-bridge-forward DC–DC converter for a residential microgrid application," *IEEE Trans. Power Electron.*, vol. 28, no. 4, pp. 1728–1740, Apr. 2013.

[5] A. Chub, D. Vinnikov, R. Kosenko, L. Liivik, and I. Galkin, "Bidirectional DC-DC converter for modular residential battery energy storage systems," *IEEE Trans. Ind. Electron.*, vol. 67, no. 3, pp. 1944–1955, Mar. 2020.

[6] "Power generation system and inverter for feeding power into a three-phase grid," U.S. Patent US8779630 (B2), Mar. 2009.

[7] "Method for checking a separation point of a photovoltaic inverter, and photovoltaic inverter," U.S. Patent US9494659 (B2), Jun. 2012.

[8] "Detection of welded switch contacts in a line converter system," U.S. Patent US20110298470 (A1), Dec. 2011.

[9] Y. Kishida, K. Koyama, H. Sasao, N. Maruyama, and H. Yamamoto, "Development of the high speed switch and its application," in *Proc. IEEE Ind. Appl. Conf.*, vol. 3, Oct. 1998, pp. 2321–2328.

[10] J. Meyer and A. Rufer, "A DC hybrid circuit breaker with ultra-fast contact opening and integrated gate-commutated thyristors (IGCTs)," *IEEE Trans. Power Del.*, vol. 21, no. 2, pp. 646–651, Apr. 2006.

[11] "A hybrid circuit breaker," European Patent EP2489053 (B1), Oct. 2009.

[12] C. Meyer, M. Kowal, and R. W. De Doncker, "Circuit breaker concepts for future high-power DC-applications," in *Proc. Ind. Appl. Conf.*, vol. 2, Oct. 2005, pp. 860–866.

[13] J. Hafner and B. Jacobson, "Protective hybrid HVdc breakers—A key innovation for reliable HVdc grids," in *Proc. CIGRE Int. Symp.*, Sep. 2011, pp. 1–8.

[14] C. Peng, X. Song, A. Q. Huang, and I. Husain, "A medium-voltage hybrid DC circuit breaker—Part II: Ultrafast mechanical switch," *Trans. Emerg. Sel. Topics Power Electron.*, vol. 5, no. 1, pp. 289–296, Mar. 2017.

[15] X. Song, C. Peng, and A. Q. Huang, "A medium-voltage hybrid DC circuit breaker, part I: Solid-state main breaker based on 15 kV SiC emitter turn-off thyristor," *Trans. Emerg. Sel. Topics Power Electron.*, vol. 5, no. 1, pp. 278–288, Mar. 2017.
[16] C. Peng, A. Q. Huang, and X. Song, "Current commutation in a medium voltage hybrid DC circuit breaker using 15 kV vacuum switch and SiC devices," in *Proc. IEEE APEC*, Mar. 2015, pp. 2244–2250.
[17] "HVDC hybrid circuit breaker with snubber circuit," U.S. Patent US8891209 (B2), Nov. 2011.
[18] "Hybrid dc circuit breaking device," U.S. Patent US20150022928 (A1), Dec. 2012.
[19] "High-voltage dc circuit breaker apparatus," European Patent EP0108279 (B1), Oct. 1983.
[20] R. Lazzari and L. Piegari, "Design and implementation of LVDC hybrid circuit breaker," *IEEE Trans. Power Electron.*, vol. 34, no. 8, pp. 7369–7380, Aug. 2019.
[21] X. Pei, O. Cwikowski, A. C. Smith, and M. Barnes, "Design and experimental tests of a superconducting hybrid DC circuit breaker," *IEEE Trans. Appl. Supercond.*, vol. 28, no. 3, pp. 1–5, Apr. 2018.
[22] "Commutation type DC breaker," U.S. Patent US5452170A, Feb. 1992.
[23] D. Jovcic, "Series LC DC circuit breaker," *IET High Voltage*, vol. 4, no. 2, pp. 130–137, Jul. 2019.
[24] "Device and method for switching a direct current," U.S. Patent US20160300671 (A1), Nov. 2013.
[25] R. Ma *et al.*, "Investigation on arc behavior during arc motion in air DC circuit breaker," *IEEE Trans. Plasma Sci.*, vol. 41, no. 9, pp. 2551–2560, Sep. 2013.
[26] Y. Kim and H. Kim, "Modeling for series arc of DC circuit breaker," *IEEE Trans. Ind. Appl.*, vol. 55, no. 2, pp. 1202–1207, Mar./Apr. 2019.
[27] T. McDonald, M. Soldano, A. Murray, and T. Avram, "Power MOSFET avalanche design guidelines," International Rectifier Application Note, AN-1005, Oct. 2004.
[28] J. S. Morton, "Circuit breaker and protection requirements for DC switchgear used in rapid transit systems," *IEEE Trans. Ind. Appl.*, vol. IA-21, no. 5, pp. 1268–1273, Sep. 1985.
[29] D. Salomonsson, L. Soder, and A. Sannino, "Protection of low-voltage DC microgrids," *IEEE Trans. Power Del.*, vol. 24, no. 3, pp. 1045–1053, Jul. 2009.
[30] S. Beheshtaein, R. Cuzner, M. Savaghebi, and J. M. Guerrero, "Review on microgrids protection," *IET Gener. Transmiss. Distrib.*, vol. 13, no. 6, pp. 743–759, Mar. 2019.

**Ken King Man Siu** (Member, IEEE) received the B.Eng. and M.Eng. degrees in electronic engineering from the City University of Hong Kong, Kowloon, Hong Kong, in 2010 and 2011, respectively, and the Ph.D. degree from the University of Manitoba, Winnipeg, Canada, in 2019.

From 2011 to 2015, he was a System Application Engineer with Infineon Technologies Hong Kong Ltd., Pak Shek Kok, Hong Kong, to evaluate the latest power semiconductors and develop their application platforms. He is currently a Postdoctoral Fellow with the Electrical and Computer Engineering Department, University of Manitoba, to research on grid-connected power electronics converters, microgrid technique, and renewable energy applications.

**Carl Ngai Man Ho** (Senior Member, IEEE) received the B.Eng. and M.Eng. double degrees and the Ph.D. degree in electronic engineering from the City University of Hong Kong, Kowloon, Hong Kong, in 2002 and 2007, respectively.

From 2002 to 2003, he was a Research Assistant with the City University of Hong Kong. From 2003 to 2005, he was an Engineer with E.Energy Technology Ltd., Hong Kong. In 2007, he joined ABB Switzerland, where he has been appointed as Principal Scientist and has led a research project team to develop solar inverter technologies. In 2014, he joined the University of Manitoba, Winnipeg, Canada, where he is currently an Associate Professor and Canada Research Chair in Efficient Utilization of Electric Power. He established the Renewable-Energy Interface and Grid Automation (RIGA) Lab, University of Manitoba, to research on microgrid technologies, renewable energy interfaces, real-time digital simulation technologies, and demand-side control methodologies.

Dr. Ho is currently an Associate Editor for the IEEE TRANSACTIONS ON POWER ELECTRONICS (TPEL) and the IEEE JOURNAL OF EMERGING AND SELECTED TOPICS IN POWER ELECTRONICS (JESTPE). He was the Second Place Winner for 2018 Prize Paper Awards of TPEL and the recipient of the Associate Editor Awards of JESTPE in 2018 and 2020.

**Dong Li** (Student Member, IEEE) received the B.Sc. degree in electrical engineering and the B.Admin. dual degrees from Tianjin University, Tianjin, China, in 2015. He is currently working toward the Ph.D. degree in electrical engineering with the University of Manitoba, Winnipeg, Canada.

He is currently a Research Assistant with the Laboratory of Renewable-Energy Interface and Grid Automation, Department of Electrical and Computer Engineering, University of Manitoba. His research interests include renewable energy interfaces, modular power electronic converters, and microgrid technologies.